Journal of Pharmacological and Toxicological Methods xxx (2016) xxx–xxx

Contents lists available at ScienceDirect

Journal of Pharmacological and Toxicological Methods

journal homepage: www.elsevier.com/locate/jpharmtox

Research article

Use of FDSS/μCell imaging platform for preclinical cardiac electrophysiology safety screening of compounds in human induced pluripotent stem cell-derived cardiomyocytes

Haoyu Zeng *, Maria I. Roman, Edward Lis, Armando Lagrutta, Frederick Sannajust

SALAR, Safety & Exploratory Pharmacology Department, Merck Research Laboratories, West Point, PA 19486, USA

ARTICLE INFO

Article history:
Received 29 February 2016
Received in revised form 6 May 2016
Accepted 18 May 2016
Available online xxxx

Keywords:
hiPSC-CM
Preclinical cardiac safety
Ca^{2+}-transient

ABSTRACT

FDSS/μCell is a high-speed acquisition imaging platform (Hamamatsu Ltd., Hamamatsu, Japan) that allows for simultaneous high-throughput reading under controlled conditions. We evaluated the Ca^{2+} transients or optical membrane potential changes of human induced pluripotent stem cell-derived cardiomyocytes (hiPSC-CMs) (iCells) in the presence or absence of 44 pharmacological agents known to interfere with cardiac ion channels (e.g., hERG, I_{Ks}, $NaV_{1.5}$, $CaV_{1.2}$). We tested two Ca^{2+}-sensitive fluorescence dyes (Codex ACTOne® and EarlyTox®) and a membrane potential dye (FLIPR® membrane potential dye). We were able to quantify and report drug-induced early-after depolarizations (EAD)-like waveforms, cardiomyocyte ectopic beats and changes in beating rate from a subgroup of pharmacological agents acting acutely (within a 1-hour period). Cardiovascular drugs, such as dofetilide and D,L-sotalol, exhibited EAD-like signals at 3 nM and 10 μM, respectively. CNS drugs, such as haloperidol and sertindole, exhibited EAD-like signals and ectopic beats at 30 nM and 1 μM, respectively. Other drugs, such as astemizole, solifenacin, and moxifloxacin, exhibited similar arrhythmias at 30 nM, 3 μM and 300 μM, respectively. Our data suggest that the membrane potential and intracellular Ca^{2+} signal are tightly coupled, supporting the idea that the EAD-like signals reported are the accurate representation of an EAD signal of the cardiac action potential. Finally, the EAD-like Ca^{2+} signal was well correlated to clinically-relevant concentrations where Torsade de Pointes (TdPs) arrhythmias were noted in healthy volunteers treated orally with some of the compounds we tested, as reported in PharmaPendium®.

1. Introduction

Drug-induced pro-arrhythmic effects have been a safety concern during drug discovery and development, and it is one of the leading causes of drug development setback and withdrawal (Laverty et al., 2011). Since the first successful generation in 2007 of induced pluripotent stem cells (iPSCs) from adult human fibroblasts (Takahashi et al., 2007), human induced pluripotent stem cell-derived cardiomyocytes (hiPSC-CMs) have recently emerged as a new and promising tool to predict proarrhythmic side-effect of drug candidates (Cerignoli et al., 2012; Guo et al., 2011; Guo et al., 2013; Lu et al., 2015; Peters, Lamore, Guo, Scott, & Kolaja, 2014; Sirenko et al., 2013), due to their close similarity to native human cardiomyocytes with expression of all major cardiac ion channels (Ma et al., 2011; Saric, Halbach, Khalil, & Er, 2014). Cardiovascular safety investigations have studied the ability of cultured hiPSC-CMs to predict the potential of a drug to cause QT interval prolongation, a risk factor for the fatal arrhythmia *Torsade de Pointes* (TdPs). For instance, electrophysiological endpoints, such as the action potential and the field potential duration, a surrogate for the QT interval, have been measured in microelectrode arrays, a label-free monitoring platform (Nozaki et al., 2014). FDSS/μCell is a high-speed acquisition imaging platform (Hamamatsu Ltd., Hamamatsu, Japan) that allows for simultaneous high-throughput reading of fluorescent signals under controlled physiological temperature (37 ± 0.1 °C). We evaluated the Ca^{2+} transients of hiPSC-CMs (iCells from CDI, Madison, MI, USA) in the presence or absence of 44 pharmacological agents known to interfere with the 4 major cardiac ion channels (e.g., hERG, I_{Ks}, $NaV_{1.5}$, and $CaV_{1.2}$). A Ca^{2+}-sensitive fluorescence dye (Codex ACTOne®, Codex BioSolutions, Gaithersburg, MD, USA) and a membrane potential dye (FLIPR® membrane potential dye, Molecular Devices, Sunnyvale, CA, USA) were tested. We were able to detect, quantify and report drug-induced early-after depolarization (EAD)-like waveforms, cardiomyocyte ectopic beats, changes in beating rate, and peak amplitude from a variety of agents. Our data, comparing the membrane potential and the intracellular Ca^{2+} signal, suggest that the EAD-like Ca^{2+} signal is tightly coupled to EADs signals and could potentially be a fast and reliable readout of EAD. Further, the data reported using FDSS/μCell platform would predict a risk for arrhythmias at therapeutic concentrations at which some of these agents are classified as torsadogenic in the clinic.

* Corresponding author at: 770 Sumneytown Pike, WP81-2216, West Point, PA 19486, USA.
E-mail address: haoyu.zeng@merck.com (H. Zeng).

http://dx.doi.org/10.1016/j.vascn.2016.05.009
1056-8719/

2. Methods

2.1. Experimental procedure

Human iPSC-CM from Cellular Dynamics International (iCells®, CDI, Madison, WI) were thawed according to the manufacture's instruction and plated in 96-well plates (ACEA-Biosystems Inc., San Diego, CA, USA) that had been pre-coated with fibronectin (50 μg/ml) for 3 h at 37 °C at a density of 30,000 cells/well. Cells were cultured for 48 h in plating media and, after that, switched to maintenance media provided by the vendor. Maintenance media was changed every other day and 24 h prior to the day of the experiment. Cells were used 14-days after plated at which time they formed a spontaneously beating monolayer. On experiment day, cells were incubated with Codex ACTOne® dye, EarlyTox® dye, or FLIPR® membrane potential dye prepared according to respective manufacturers' instructions extemporaneously prior to use, for 1 h at 37 °C, 5% CO_2. Light source (L11601–01) was used with an output excitation wavelength of 480 nm and an emission of 540 nm. FDSS/μCell imaging platform (Hamamatsu Ltd., Hamamatsu, Japan) simultaneously collected Ca^{2+} transient signals from 96-well plates, at a sampling rate of 16 Hz, except otherwise indicated, for 1 min. hiPSC-CMs culture plates were maintained at 37 °C during the acquisition time.

2.2. Test compound formulations

All test standards were purchased from Sigma-Aldrich (St. Louis, MO, USA). Stock solutions of the test compounds were prepared in 100% DMSO, and serially diluted 1:1000 into compound plate for testing (0.1% DMSO was the maximum concentration in all wells). Measurements were taken during pretest, and approximately 15-min, 30-min, 1-h post-treatment. All compounds were tested in triplicate ($n = 3$ wells/concentration). Time-matched vehicle (0.1% DMSO) wells were included in every plate to correct for any time-and/or vehicle-dependent effect on the parameters measured. Concentrations of test compounds in cell culture media were not confirmed analytically.

2.3. Data analysis

Raw Ca^{2+} transient signals were analyzed via the use of the waveform analysis software provided by the vendor for determination of peak counts (beating rates), peak amplitudes and peak width durations at 80% (CTD80). Raw traces and analysis results were integrated with Pipeline Pilot® and visualized with Spotfire®. EADs were not quantified, but visually identified as illustrated in Fig. 2B. Data recorded prior to and for each successive time-points after test compound addition were reported as average of 1-min period of recording. Each compound was tested at four different ascending concentrations in triplicate, with $n = 1$ concentration/well without any sequential additions. Data of each well were normalized to pre-read (pre-drug administration) of that well, corrected with time-matched 0.1% DMSO control, and then averaged. All final results are shown as mean ± SEM (standard error of mean), except otherwise indicated. The assay sensitivity, specificity, and predictivity used in this study were defined and calculated as follows:

$$\text{Sensitivity} = TP/(TP + FN)$$

$$\text{Specificity} = TN/(TN + FP)$$

$$\text{Predictivity} = (TP + TN)/(TP + FN + TN + FP)$$

True positive (TP) = clinically-observed TdPs; true negative (TN) = no clinical TdPs; false positive (FP) = EADs in this assay but not confirmed by clinical observation; false negative (FN) = fail to detect drugs that cause TdPs clinically.

3. Results

We first performed a time course experiment to evaluate the integrity of Codex ACTOne® and EarlyTox® Ca^{2+} dyes, claimed to be nontoxic by their manufacturers. hiPSC-CMs were incubated for 1 h, with either dye. The first reading was conducted at Time 0 (which is 1 h after the dye incubation time), using the FDSS/μCell imaging platform. As shown in Fig. 1, at approximately 1 h after the first reading, Codex ACTOne® dye showed a small effect on beating rate and peak amplitude that was considered minimal, up to 1.5 h. Beating rate remained relatively stable up to 3.5 h while the peak amplitude progressively decreased over time. In comparison, time course of EarlyTox® dye showed a significant and time-dependent increase in peak amplitude that was >350% change at the end of 4 h, while the beating rate progressively decreased over time. Both dyes were nontoxic to iCells, as beating rate was still detected after overnight incubation (data not shown). Based on these results, we determined that the Codex ACTOne® dye was an optimal dye to use with iCells and the FDSS/μCell imaging platform, and we adjusted our incubation time to be 1.5 h, prior to Time 0 reading.

Then, we determined if the Ca^{2+}-transient measurements collected by our system were able to detect any pro-arrhythmic effects of several reference pharmacological agents. As an example, dofetilide, a well-known TdPs-inducer drug, exhibited a clear EAD-like concentration response after ~10-min incubation period, with more pronounced pro-arrhythmic patterns at higher concentrations (Fig. 2A). In this assay, we measured peak amplitude and peak count (i.e., beating rate), Ca^{2+} transient duration (CTD) at 80% position of repolarization (CTD80), considered a surrogate for the QT interval of the electrocardiogram, and EAD-like Ca^{2+} signals (Fig. 2B). We found that cardiovascular drugs such as dofetilide and D,L-sotalol produced EAD-like signals at 3 nM and

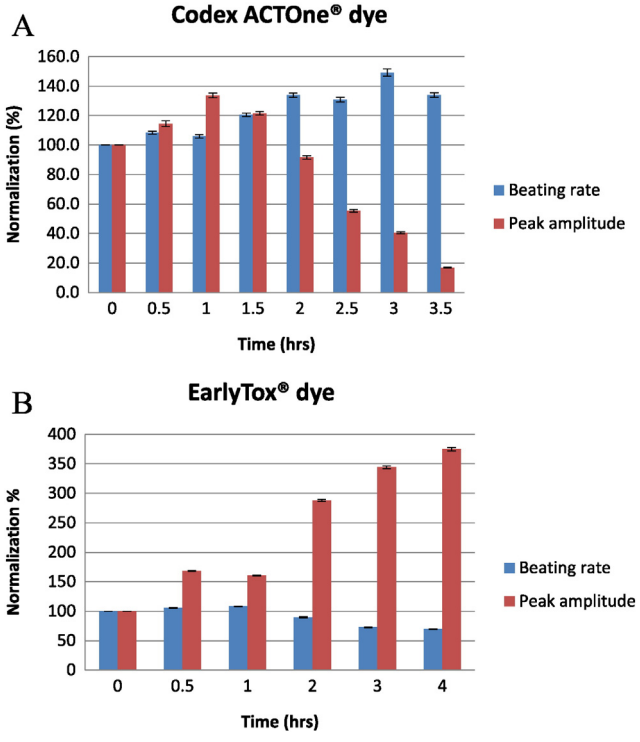

Fig. 1. Time course with different Ca^{2+} dyes. Identical experimental procedure was used in both dye time course studies. A: Codex ACTOne® dye; B: EarlyTox® dye. Due to differences in the local environment for each well (i.e., slight difference in viable cell number, cell health, respective beating rate of "pacemaker" cells), the beating rate and absolute amplitude of Ca^{2+} transient can vary from well to well: at T = 0, the beating rate (beats/min), and the absolute amplitude (absolute units) of the plates shown in A and B are: 25 ± 3 and 8630 ± 1733 (mean ± standard deviation, n = 92); and 24 ± 2 and 9002 ± 936 (mean ± standard deviation, n = 96), respectively.

Please cite this article as: Zeng, H., et al., Use of FDSS/μCell imaging platform for preclinical cardiac electrophysiology safety screening of compounds in human induced pluri..., *Journal of Pharmacological and Toxicological Methods* (2016), http://dx.doi.org/10.1016/j.vascn.2016.05.009

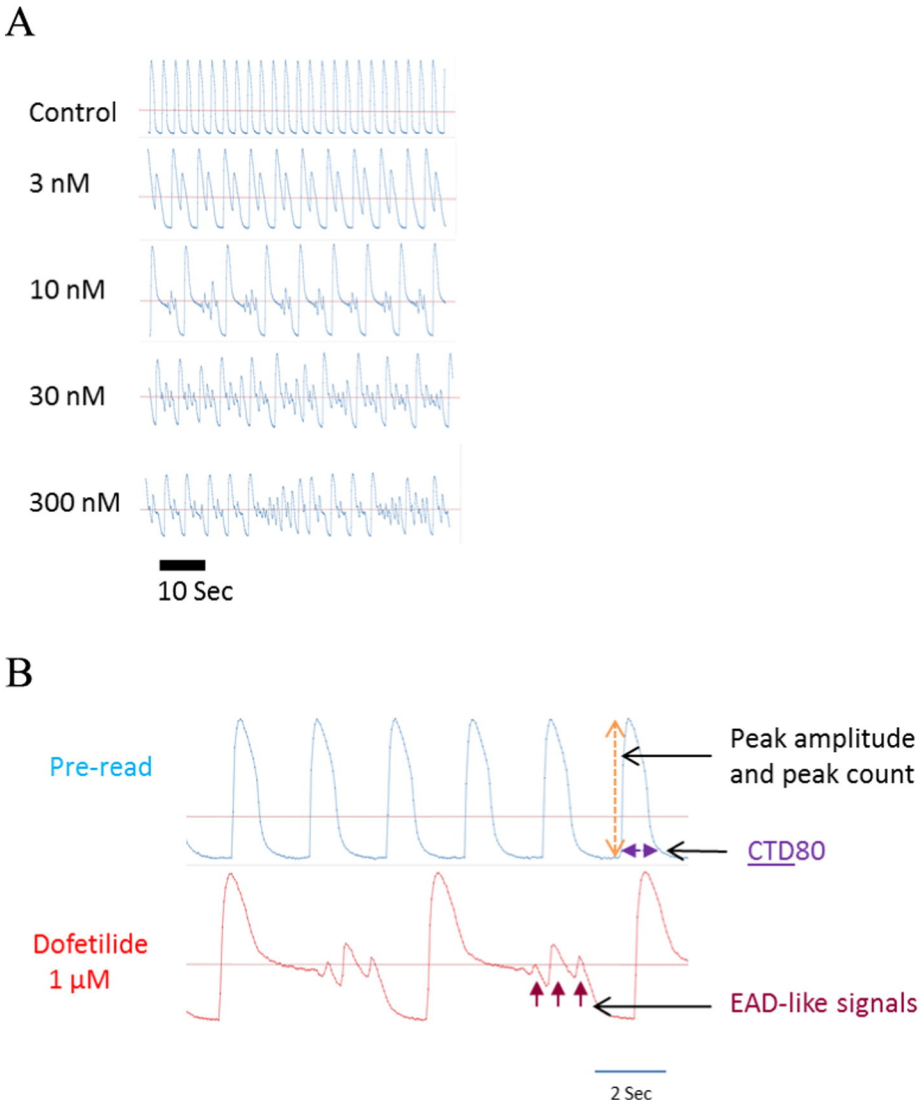

Fig. 2. Ca^{2+} transient measurement. A: Representative Ca^{2+} transient traces of vehicle control and 30 min after addition of different concentrations (3, 10, 30 and 300 nM) of dofetilide. B: Parameters measured in the Ca^{2+} transient signal were: peak amplitude and peak count; CTD80; and EAD-like signals (data were acquired at 110 Hz).

10 µM, respectively. CNS drugs, such as haloperidol and sertindole, produced EAD-like signals and ectopic beats at 30 nM and 1 µM, respectively. Other agents, such as, astemizole, solifenacin and moxifloxacin, produced similar arrhythmias at 30 nM, 3 µM and 300 µM, respectively. We observed that the EAD-like signals were usually preceded by prolongation of the CTD80 parameter, e.g. solifenacin exhibited a 36% increase in CTD80 (compared to baseline) at 300 nM (Table 1).

We investigated if the EAD-like signal observed with Ca^{2+}-transient measure was indeed an EAD-related signal. We applied both Codex ACTOne® Ca^{2+} dye and FLIPR® membrane potential dye to the same wells of cells to acquire Ca^{2+} signal and membrane potential from same cells for signal correlation. As shown in Fig. 3, within a single well, and in response to different drug classes (cisapride, verapamil, FPL64176, isoproterenol, and ivabradine), EAD-like signals detected by monitoring Ca^{2+} transients were equivalent to membrane potential signals evoked from the same cells.

Finally, using EAD-like signal as readout, we evaluated the effects of 44 pharmacological agents including 24 positive standards that caused TdPs clinically, to examine the predictability of our assay for clinical TdPs (Table 2). With this test set, we identified 20 true positive (TP), 17 true negative (TN), 4 false negative (FN) and 3 false positive (FP) drugs (detail in Table 2). Therefore, our assay has 83% sensitivity, 85% specificity, and an overall 84% predictivity. We were also able to represent, for 12 of the reference pharmacological agents, the clinical plasma concentrations at which TdPs were clinically-reported in PharmaPendium® against their respective EAD concentrations observed in our assay. The correlation showed that 75% data points were within 10× fold range defined by lines (Fig. 4).

4. Discussion

Ca^{2+} transients (i.e., rises and reductions of cytosolic Ca^{2+} concentrations) regulate the contraction and relaxation cycles that are followed by the action potential in cardiac myocytes. In this report, we demonstrated that by monitoring Ca^{2+} signals (spikes and waves) with Ca^{2+}-sensitive dyes, we obtained reliable information about drug effects on the action potential. Similarly, when membrane potential dyes were evaluated, action potential signals elucidated changes induced by the drug. Our data suggest that the membrane potential and the intracellular Ca^{2+} signal are tightly coupled, supporting the idea that EAD-like signals acquired with Ca^{2+} dye are an accurate representation of an EAD signal of the cardiac action potential.

Because our assay relies on an invasive detection method, dye selection plays a critical role, especially in light of the cytotoxic properties of some dyes, such as Fluo-4 and Calcium-5 (application note from Molecular Devices). The non-cytotoxic EarlyTox® dye continuously increased

Please cite this article as: Zeng, H., et al., Use of FDSS/µCell imaging platform for preclinical cardiac electrophysiology safety screening of compounds in human induced pluri..., *Journal of Pharmacological and Toxicological Methods* (2016), http://dx.doi.org/10.1016/j.vascn.2016.05.009

Table 1
Ca^{2+} transient data of 12 reference pharmacological agents. When EAD-type signal was observed ("yes"), the peak count, peak amplitude and CDT80 parameters were excluded.

Compound	Concentration (nM)	Beating rate change (%)		Peak amplitude change (%)		CTD80 change (%)		Observed EAD-type signal	TdP clinical Cmax (nM)
		Mean	SEM	Mean	SEM	Mean	SEM		
Astemizole	0.3	97.9	0.1	105.3	2.5	100.8	1.3		
	1	95.6	4.3	99.6	0.1	115.5	3.6		
	3	92.2	4.2	104.4	1	107.9	2.2		
	30	–	–	–	–	–	–	Yes	4.7
Bepridil	37	112.6	2.5	97.4	4.1	91.1	0.1		
	111	105.2	2.6	96.2	3.9	98.9	1.1		
	333	99.4	1.3	96.4	3.5	108.9	1.5		
	1000	–	–	–	–	–	–	Yes	2200
Cisapride	3	94.5	0	106.9	1	101.7	0.4		
	10	89.9	2.3	104.9	3.3	106.1	3.9		
	30	88	3.1	98.2	1.3	112.8	4.3		
	300	–	–	–	–	–	–	Yes	68
Dofetilide	3	–	–	–	–	–	–	Yes	
	10	–	–	–	–	–	–	Yes	
	30	–	–	–	–	–	–	Yes	
	300	–	–	–	–	–	–	Yes	8.9
Dolasetron	1111	101.8	0.5	98.8	4.4	–	–		
	3333	96.9	0.5	103.8	19.2	–	–		
	10,000	–	–	–	–	–	–	Yes	
	30,000	–	–	–	–	–	–	Yes	540
Flecainide	300	78.6	3.7	99.4	1.1	123.6	5.9		
	1000	–	–	–	–	–	–	Yes	
	3000	–	–	–	–	–	–	Yes	
	30,000	–	–	–	–	–	–	Stop beating	400
Haloperidol	10	90.8	2.1	105.4	0.4	109.6	1.1		
	30	80.7	1.3	96.1	1.3	142.2	0.8		
	100	74.6	0.9	93	2.4	145.5	0.7		
	1000	–	–	–	–	–	–	Yes	23
Ketoconazole	1111	96.4	3.1	116.4	14.4	108.9	3.5		
	3333	95.2	6.9	166	19.3	82.7	40.7		
	10,000	–	–	–	–	–	–	Yes	
	30,000	–	–	–	–	–	–	Yes	6600
Moxifloxacin	3000	96.9	3.1	102.8	3.6	100.6	4.3		
	10,000	89.9	2.3	105.2	2.1	108.1	3.1		
	30,000	82.3	3.1	105.8	3.2	117.2	2.4		
	300,000	–	–	–	–	–	–	Yes	7100
Solifenacin	30	89.2	6.3	100.6	0.7	109.1	2.1		
	100	87	5.2	103.6	1.5	117.5	3.2		
	300	69.5	3	97.3	1.6	136.3	3.6		
	3000	–	–	–	–	–	–	Yes	67
Sotalol	1000	98.4	9.6	93	11.8	78.1	39.6		
	10,000	–	–	–	–	–	–	Yes	
	100,000	–	–	–	–	–	–	Yes	1800
Terodiline	1111	–	–	–	–	–	–	Yes	
	3333	–	–	–	–	–	–	Yes	
	10,000	–	–	–	–	–	–	Stop beating	
	30,000	–	–	–	–	–	–	Stop beating	5.9

peak amplitude (to >350% change), and it also reduced beating rate over time. In comparison, the Codex ACTOne® dye maintained relatively stable peak amplitudes that can easily be corrected with time-matching vehicle controls (same plate, different wells). We observed a marked decrease in peak amplitude after 1.5 h that is mainly due to efflux of the dye, which can be prevented by the addition of 1 mM probenecid. We observed that peak amplitudes were stable within the 1-hour test-window of our assay. For this reason, we decided not to use probenecid. Pronounced decreases in amplitude appeared to be compound-dependent, as evidenced by the concentration response of the various standards tested (e.g., Fig. 3A & B). We cannot exclude compound-dye interaction, photo-bleaching, or an actual reduction in membrane potential amplitude. Aware of variations in the peak amplitude parameter, we limited monitoring to time-points with little or no amplitude variation in control experiments (Fig. 1) and corrected signals against time-matched vehicle controls. In addition, we focused our investigation on detection of EAD-like signals and CTD80 increases, and not on signal amplitude changes.

It is not surprising to observe that the Ca^{2+} transient signal is well-correlated to the membrane potential signal of the same cells, during control period and in the presence of different agents, since it is well-established that EAD is carried by cytoplasmic Ca^{2+} ions (January & Moscucci, 1992; Qu et al., 2013). The well-matched morphology between membrane potential and Ca^{2+} signals in the presence of hERG blocker (cisapride), CaV1.2 blocker (verapamil), CaV1.2 enhancer (FPL64176), pace-maker blocker (ivabradine) and beta-adrenergic agonist (isoproterenol) clearly confirmed the accuracy of our analysis when reporting drug-induced EAD-like waveforms. Our data also suggest that the membrane potential and intracellular Ca^{2+} signal are tightly coupled, supporting the idea that the intracellular Ca^{2+} EAD-like fluctuations report accurately the represented EAD signals of the cardiac action potential.

During the study, CTD80 prolongation was always observed prior to appearance of EADs. Therefore, EAD was the end-point of this assay and CTD80 was a predictive indicator of EAD and can be used for structure-activity relationship. The specific case of astemizole that is known to prolong QT in the clinic in more dramatic fashion than we show here, is complicated by the fact that the active circulating metabolite desmethyl-astemizole, after repeat dosing, may be impacting the clinically-detected effect (Vorperian et al., 1996). The effects of potentially-

Please cite this article as: Zeng, H., et al., Use of FDSS/μCell imaging platform for preclinical cardiac electrophysiology safety screening of compounds in human induced pluri..., *Journal of Pharmacological and Toxicological Methods* (2016), http://dx.doi.org/10.1016/j.vascn.2016.05.009

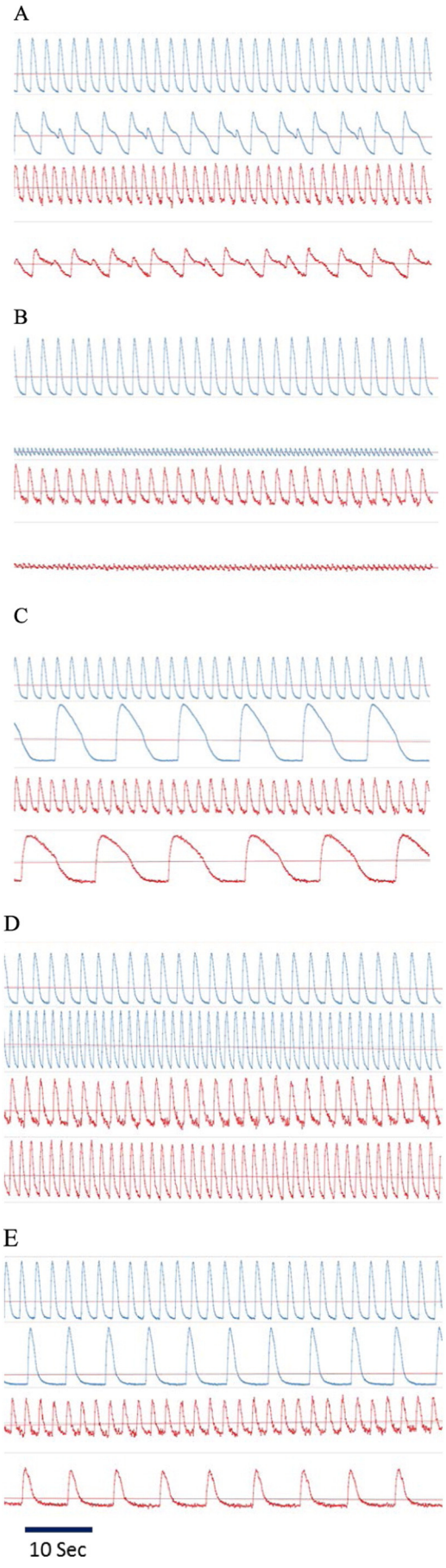

active metabolites are beyond the scope of this study, focusing mainly on the acute effects of reference pharmacological agents.

According to the test-set of 44 known pharmacological agents, our assay has 83% sensitivity, 85% specificity, and 84% predictivity. Among the four FN drugs, terfenadine caused TdPs clinically only when co-administrated with ketoconazole or in patients with congenital QT interval prolongation. Probucol caused TdPs at a delayed time-point, implying indirect, chronic effects. Both scenarios are out-of the scope of this direct, acute measurement. Similarly, the apparent discrepancy between amiodarone and dronedarone (amiodarone-derivative) causing TdPs clinically, but not generating EADs at up to 30 μM in our assay, remains unexplored. Among the three FP, ivabradine and tolterodine both caused adverse cardiac effects, although no TdPs has been reported; while ranolazine caused EADs in our assay without any evidence of TdPs in the patients. It is well-established that, in clinic, ivabradine blocks If current to slow heart rate, which is confirmed by this assay. We can speculate that EADs observed with ivabradine at high concentrations may be related to the expression of If current throughout the syncytium, without structurally-separated pacemaking system, and responsive hiPSC-CMs that appear quiescent and refractory. Moxifloxacin clinically causes QT prolongation, and corresponds in this assay to detectable CTD80 prolongation with calcium dye, and action potential prolongation with membrane dye. We do not really understand why prolongation induces EADs in our system. Rare cases of QT prolongation by therapeutically-relevant doses of moxifloxacin, associated with TdPs, have been reported in the clinic (e.g. Altin et al., 2007; Sherazi, DiSalle, Daubert, & Shah, 2008). Limited by our current dataset, we could not explain the discrepancy of effects of ranolazine that induced EADs in iCells, but no clinical TdPs. We speculated that it might be a phenotype if iCell may lack functional late-Na^+ currents.

We were able to identify clinical plasma concentrations at which TdPs was reported in PharmaPendium® only for 12 of the torsadogenic drugs tested as part of our set of reference pharmacological agents. Since our assays were conducted in the presence of serum, we correlated total concentrations at which EAD signals were detected without correction for any plasma protein binding factor, with the reported clinical torsadogenic concentrations. In this correlation, the EAD-like signal from Ca^{2+} transient assay was well-matched to clinically-reported TdPs concentrations.

Due to its featured high-speed camera, FDSS/μCell system can provide a maximal sampling rate of 110 Hz (Fig. 2B), a clear advantage over comparable platforms (e.g., FLIPR system which have a lower sampling rate of 8 Hz) that may not provide enough resolution to acquire Ca2+ transient signals from spontaneously beating hiPSC-CMs. We observed that a 16 Hz sampling rate was sufficient to capture all signals and appropriate for adequate data processing in this study, because the iCell syncytia had beating rates of approximately ~0.5 Hz, as shown in Figs. 2 and 3. Therefore, we selected to use a 16 Hz-sampling rate, except for data in Fig. 2B.

Data obtained using our FDSS/μCell system are comparable with recent Ca^{2+} transient assay using high content kinetic image cytometry (KIC) (Cerignoli et al., 2012; Lu et al., 2015). The FDSS/μCell platform allows data collection from each well simultaneously (from both 96- or 384-well formats) with data acquisition times extendable to tens of minutes. In contrast, data reported using the KIC system were recorded sequentially, one well at a time in a 48-well format, limiting acquisition time to few seconds, possibly introducing time-dependent variation, and not suitable for longer time monitoring. However, the KIC system

Fig. 3. Ca^{2+} transient and membrane potential correlation. Representative traces of $Ca2^{+}$ transient signals (blue) and membrane potential signals (red) in the presence of drugs (A: 100 nM cisapride; B: 300 nM verapamil; C: 300 nM FPL64176; D: 100 nM isoproterenol; and E: 300 nM ivabradine). Values were normalized to its respective pre-read signal (represented by top traces within each respective color). Same time scale is represented for all panels - as shown in E. (For interpretation of the references to color in this figure legend, the reader is referred to the web version of this article.)

Please cite this article as: Zeng, H., et al., Use of FDSS/μCell imaging platform for preclinical cardiac electrophysiology safety screening of compounds in human induced pluri..., *Journal of Pharmacological and Toxicological Methods* (2016), http://dx.doi.org/10.1016/j.vascn.2016.05.009

Table 2
Data correlation: EADs vs. clinical TdPs.

Outcomes	No clinical TdPs	Clinical TdPs
Ca^{2+} transient	True negative^{TN}	False negative^{FN}
No EADs	17	4
Ca^{2+} transient	False positive^{FP}	True positive^{TP}
EADs	3	20

TN: adenosine, alfuzosin, amantadine, amiloride, amlodipine, chromanol293, diltiazem, flunarizine, glyburide, indapamide, ioxynil, lidocaine, minoxidil, nicorandil, nifedipine, sildenafil, verapamil, and ioxynil.
FN: terfenadine: evidence of TdPs when co-administered with ketoconazole or congenital QT prolongation, probucol: chronic effect (evidence of delayed QT and TdPs), amiodarone: TdPs in the clinic, dronedarone (amiodarone-like): TdPs in the clinic.
FP: ivabradine and tolterodine both caused adverse cardiac effects although no TdPs have been reported, ranolazine had no evidence of TdPs in clinic.
TP: astemizole, bepridil, cisapride, dofetilide, dolasetron, flecainide, fluoxetine, haloperidol, ketoconazole, mallotoxin, moxifloxacin, nilotinib, oubain, pentamidine, pimozide, quinidine, sertindole, solifenacin, sotalol, and terodiline.

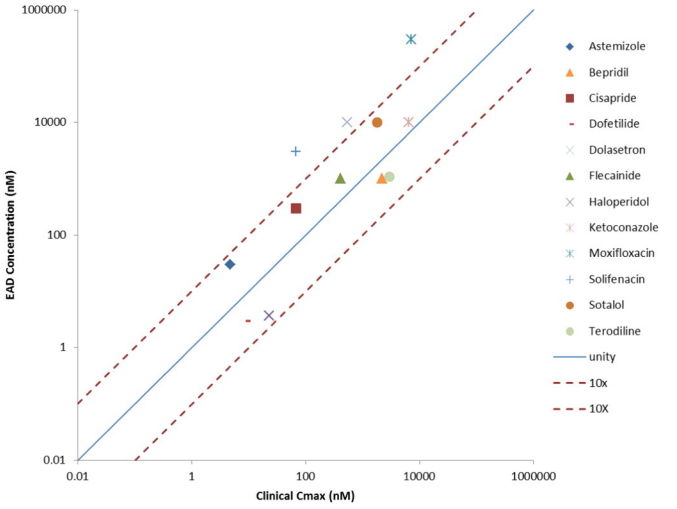

Fig. 4. EAD concentration and clinical TdPs concentration correlation. Known clinical concentrations at which TdPs were reported for twelve torsadogenic drugs are plotted as function of the lowest concentrations at which EADs was observed in the Ca^{2+} transient assay. The "blue" solid line indicates ideal 1:1 correlation and the two dashed lines indicate theoretical 10× shifted correlations; these lines are included to assess correlation quality between preclinical and clinical concentrations, overall and for each one of the drugs. (For interpretation of the references to color in this figure legend, the reader is referred to the web version of this article.)

can provide individual cell level information that is beyond the capacity of our FDSS/μCell system.

In summary, monitoring Ca^{2+} transient parameters and morphology of Ca^{2+} and membrane potential signals allowed us to elucidate EADs and potential risk for arrhythmias. In this manner, we were able to reliably predict the proarrhythmic cardiac effect(s) of diverse groups of drugs. We believe that this assay could be part of an integrated early assessment of preclinical cardiac safety evaluation, together with other assays (e.g., ion channel profiling patch-clamp studies).

References

Altin, T., Ozcan, O., Turhan, S., Ongun, O. A., Akyurek, O., Karaoguz, R., & Guldal, M. (2007). Torsade de pointes associated with moxifloxacin: A rare but potentially fatal adverse event. *The Canadian Journal of Cardiology*, *23*, 907–908.

Cerignoli, F., Charlot, D., Whittaker, R., Ingermanson, R., Gehalot, P., Savchenko, A., ... Mercola, M. (2012). High throughput measurement of Ca(2)(+) dynamics for drug risk assessment in human stem cell-derived cardiomyocytes by kinetic image cytometry. *Journal of Pharmacological and Toxicological Methods*, *66*, 246–256.

Guo, L., Abrams, R. M., Babiarz, J. E., Cohen, J. D., Kameoka, S., Sanders, M. J., ... Kolaja, K. L. (2011). Estimating the risk of drug-induced proarrhythmia using human induced pluripotent stem cell-derived cardiomyocytes. *Toxicological Sciences*, *123*, 281–289.

Guo, L., Coyle, L., Abrams, R. M., Kemper, R., Chiao, E. T., & Kolaja, K. L. (2013). Refining the human iPSC-cardiomyocyte arrhythmic risk assessment model. *Toxicological Sciences*, *136*, 581–594.

January, C. T., & Moscucci, A. (1992). Cellular mechanisms of early afterdepolarizations. *Annals of the New York Academy of Sciences*, *644*, 23–32.

Laverty, H., Benson, C., Cartwright, E., Cross, M., Garland, C., Hammond, T., ... Valentin, J. (2011). How can we improve our understanding of cardiovascular safety liabilities to develop safer medicines? *British Journal of Pharmacology*, *163*, 675–693.

Lu, H. R., Whittaker, R., Price, J. H., Vega, R., Pfeiffer, E. R., Cerignoli, F., ... Gallacher, D. J. (2015). High throughput measurement of ca^{++} dynamics in human stem cell-derived cardiomyocytes by kinetic image cytometery: A cardiac risk assessment characterization using a large panel of cardioactive and inactive compounds. *Toxicological Sciences*, *148*, 503–516.

Ma, J., Guo, L., Fiene, S. J., Anson, B. D., Thomson, J. A., Kamp, T. J., ... January, C. T. (2011). High purity human-induced pluripotent stem cell-derived cardiomyocytes: Electrophysiological properties of action potentials and ionic currents. *American Journal of Physiology. Heart and Circulatory Physiology*, *301*, H2006–H2017.

Nozaki, Y., Honda, Y., Tsujimoto, S., Watanabe, H., Kunimatsu, T., & Funabashi, H. (2014). Availability of human induced pluripotent stem cell-derived cardiomyocytes in assessment of drug potential for QT prolongation. *Toxicology and Applied Pharmacology*, *278*, 72–77.

Peters, M. F., Lamore, S. D., Guo, L., Scott, C. W., & Kolaja, K. L. (2014). Human stem cell-derived cardiomyocytes in cellular impedance assays: Bringing cardiotoxicity screening to the front line. *Cardiovascular Toxicology*.

Qu, Z., Xie, L. H., Olcese, R., Karagueuzian, H. S., Chen, P. S., Garfinkel, A., & Weiss, J. N. (2013). Early afterdepolarizations in cardiac myocytes: Beyond reduced repolarization reserve. *Cardiovascular Research*, *99*, 6–15.

Saric, T., Halbach, M., Khalil, M., & Er, F. (2014). Induced pluripotent stem cells as cardiac arrhythmic in vitro models and the impact for drug discovery. *Expert Opinion on Drug Discovery*, *9*, 55–76.

Sherazi, S., DiSalle, M., Daubert, J. P., & Shah, A. H. (2008). Moxifloxacin-induced torsades de pointes. *Cardiology Journal*, *15*, 71–73.

Sirenko, O., Crittenden, C., Callamaras, N., Hesley, J., Chen, Y. W., Funes, C., ... Cromwell, E. F. (2013). Multiparameter in vitro assessment of compound effects on cardiomyocyte physiology using iPSC cells. *Journal of Biomolecular Screening*, *18*, 39–53.

Takahashi, K., Tanabe, K., Ohnuki, M., Narita, M., Ichisaka, T., Tomoda, K., & Yamanaka, S. (2007). Induction of pluripotent stem cells from adult human fibroblasts by defined factors. *Cell*, *131*, 861–872.

Vorperian, V. R., Zhou, Z., Mohammad, S., Hoon, T. J., Studenik, C., & January, C. T. (1996). Torsade de pointes with an antihistamine metabolite: Potassium channel blockade with desmethylastemizole. *Journal of the American College of Cardiology*, *28*, 1556–1561.

Please cite this article as: Zeng, H., et al., Use of FDSS/μCell imaging platform for preclinical cardiac electrophysiology safety screening of compounds in human induced pluri..., *Journal of Pharmacological and Toxicological Methods* (2016), http://dx.doi.org/10.1016/j.vascn.2016.05.009